

The effect of anti-IL-6 receptor antibody for the treatment of Mch-Ipr/Ipr-RA1 mice that spontaneously developed destructive arthritis and enthesitis

著者	Takuya Izumiyama, Yu Mori, Shiro Mori, Naoko Mori, Tetsuya Kodama, Eiji Itoi
journal or publication title	BMC Musculoskeletal Disorders
volume	20
number	286
page range	1-12
year	2019-06-15
URL	http://hdl.handle.net/10097/00127009


doi: 10.1186/s12891-019-2664-3

RESEARCH ARTICLE

Open Access



The effect of anti-IL-6 receptor antibody for the treatment of Mch-Ipr/Ipr-RA1 mice that spontaneously developed destructive arthritis and enthesitis

Takuya Izumiyama¹, Yu Mori^{1*} , Shiro Mori², Naoko Mori³, Tetsuya Kodama² and Eiji Itoi¹

Abstract

Background: Mch-Ipr/Ipr-RA1 mice are a new strain of mice which spontaneously develop destructive arthritis and enthesitis in the ankle. There is no published data that drug treatment has been trialed on these mice. This study examined the effect of the mouse anti-IL-6 receptor antibody, MR16-1, for the treatment of arthritis and enthesitis in Mch-Ipr/Ipr-RA1 mice.

Methods: Male Mch-Ipr/Ipr-RA1 mice were randomly divided into control and treatment groups. MR16-1 was administered from 10 weeks of age for the treatment group. Saline was applied for the control group. The drug was administered once a week, at an initial dose of 2 mg, then maintained at 0.5 mg once per week thereafter. The effects were evaluated by the histopathological synovitis score, in vivo imaging using indocyanine green liposomes, and analysis of the gene expression of inflammatory cytokines.

Results: Tissue analyses were carried out at 14, 17 and 20 weeks of age. The synovitis scores of treated groups were significantly lower compared with those of the control group at 14 and 17 weeks of age. The kappa coefficient was 0.77. However, progression of enthesal ossification persisted in the MR16-1 treated group. In vivo imaging using indocyanine green liposomes showed significant decreases in signal intensities of treated groups at week 14, but no significant differences were observed at week 18. Blood serum amyloid A levels in treated groups were significantly lower at 17 weeks of age. The gene expression levels of *Tnf* and *Il17* were also significantly lower in MR16-1 treated groups.

Conclusions: Administration of the anti-IL-6 receptor antibody is effective for the treatment of synovitis and bone destruction of Mch-Ipr/Ipr-RA1 mice. Mch-Ipr/Ipr-RA1 mice may be a suitable experimental model for the development of new treatments for destructive arthritis and enthesitis. IL-6 signal blockade could contribute to the treatment of destructive arthritis, and further studies should be carried out to confirm its potential in the prevention of enthesopathy developed to ossification.

Keywords: Arthritis, Enthesitis, Anti-IL-6 receptor antibody, IMS

* Correspondence: yu-mori@med.tohoku.ac.jp

¹Department of Orthopaedic Surgery, Tohoku University Graduate School of Medicine, 1-1, Seiryō-machi, Aoba-ku, Sendai, Miyagi 980-8574, Japan
Full list of author information is available at the end of the article



Background

Autoimmune arthritis diseases with enthesal inflammation show complex pathological features, including synovitis, bone erosion, enthesitis [1]. The imbalance of bone and cartilage formation and the destruction of joint structure results in the structural changes observed in these diseases. Rheumatoid arthritis is characterized by synovial proliferation and erosion of joint cartilage due to chronic inflammation [2]. On the other hand, autoimmune arthritis with enthesal inflammation like as psoriatic arthritis involves a distinct remodeling process leading to enthesal ossification with synovial proliferation and bone erosion [3, 4]. The histological characteristics of enthesal ossification include the proliferation of cartilage formation, and subsequent replacement of cartilage by bone (endochondral ossification) [5, 6]. Recent studies have reported that IL-17 and IL-22 signaling molecules released from IL-23 positive T cells are involved in enthesal chondral proliferation and ossification [7, 8]. Patients with ossifying enthesitis are typically treated with tumor necrosis factor (TNF)- α inhibitors. However, the prevention of enthesal ossification is recognized as being difficult especially in advanced stages of the disease [9–11]. Moreover, animal models of synovitis with concomitant enthesal ossification are yet to be established. It is necessary to study animal models of synovitis with intercurrent enthesal ossification to elucidate the pathological mechanisms of the disease, and develop new treatment methods.

Our research group have previously reported the development of a murine model with spontaneous, progressive synovitis and enthesitis in ankle joints [12]. Backcross generation mice were prepared using a non-arthritis strain of mice, C3H/HeJ-lpr/lpr (C3H/lpr), MRL/lpr \times (MRL/lpr \times C3H/lpr) F1. Among these N2 mice, we observed development of arthritis of the ankle joints, with macroscopic swelling. We then began to intercross the N2 mice, by selection based on swelling of the ankle joints. Finally, we established a novel recombinant strain of mice, designated McH-lpr/lpr-RA1, which showed a high incidence of arthritis with enthesopathy. Analysis of the destructive arthritis and enthesitis processes may elucidate the fundamental mechanisms of peripheral inflammation in spondyloarthritis.

The anti-IL-6 receptor monoclonal antibody is available for clinical use in patients with rheumatoid arthritis, and has been shown to have therapeutic effects in the treatment of severe rheumatoid arthritis [13]. The effect of anti-IL-6 treatment in patients with ankylosing spondylitis has also been reported — studies revealed that the anti-IL-6 receptor antibody did not prevent the progression of spinal changes associated with ankylosis [14]. Furthermore, the effect of treatment with anti-IL-6 receptor antibody on peripheral arthritis of spondyloarthritis has also

been reported, but the study reported mainly about insufficient effects on spinal disorder and its use in enthesal inflammation and ossification with destructive arthritis remains unclear [15]. MR16–1 is a rat anti-IL-6 receptor monoclonal antibody, as previously described in the literature [16]. MR16–1 is used in many experimental disease models to assess the effects of blocking IL-6 signaling [17–23]. McH-lpr/lpr-RA1 mice may provide a suitable animal model to assess the therapeutic effects of IL-6 signal blockade in enthesal inflammation and ossification, and the administration of MR16–1 will determine the potential treatment effects of IL-6 ligand and receptor blockade.

The purpose of the present study is to investigate the effect of MR16–1 for the treatment of ankle joint arthritis with enthesopathy, and the mechanism of enthesal inflammatory change and ossification in the experimental murine model of McH-lpr/lpr-RA1 mice. We hypothesized that IL-6 signal blockade would suppress the progression of synovial proliferation and enthesal ossification in McH-lpr/lpr-RA1 mice.

Methods

Animals

McH/lpr-RA1 mice were generated using F54 C3H/HeJ-lpr/lpr and MRL/lpr \times (MRL/lpr \times C3H/lpr) mice in the animal unit of Tohoku University Medical School. This recombinant congenic strain of mice was designated McH/lpr-RA1 as previously described in the literature [12]. All mice were housed in the animal unit of Tohoku University Medical School, an environmentally controlled and specific pathogen-free facility. Animal protocols were reviewed and approved by the Tohoku University Animal Studies Committee. The animal experiments approval number of our institute was 2015-MdA-247-1. The animals were maintained in individually-ventilated cage (225 \times 338 \times 140 mm) at 22 \pm 2 $^{\circ}$ C and 40 \pm 20% humidity, receiving water and specific animal pellet-type laboratory-animal food. All experiments were performed using week 10 male mice. The mice were randomly allocated to treatment and control groups at week 10. The animals were euthanized in a carbon dioxide gas chamber at 14–20 weeks of age.

Treatment of mice

IL-6 signal blockade was performed with an intraperitoneal injection of 2 mg of rat anti-mouse IL-6R mAb (MR16–1, a kind gift from Chugai Pharmaceutical, Tokyo, Japan), once in the first treatment (week 10). Thereafter, 0.5 mg of MR 16–1 was administered once a week until 20 weeks of age as previously described in the literature [24] Phosphate buffered saline (PBS) was administered on the same schedule as a negative control.

Enzyme-linked immunosorbent assay

Serum amyloid A (SAA) and IL-6 levels were determined using an enzyme-linked immunosorbent assay (ELISA) kit for SAA and IL-6 (Biosource, Camarillo, CA and R&D Systems Inc., Minneapolis, MN, USA) according to the manufacturer’s recommendations at 14 and 17 weeks of age (*n* = 5 for each group). Briefly, serum samples were diluted 1:200 in assay diluent and incubated with conjugated anti-mouse SAA antibody. Serum samples were incubated with anti-mouse IL-6 antibody without dilution. Substrate tetramethylbenzidine was added, samples were read at OD450 nm and results were analyzed using the four-parameter fit to determine SAA values.

Histomorphometric analysis

Ankle joints were harvested at 14, 17 and 20 weeks of age and decalcified by soaking in 220 mM/L EDTA-Na for 3 weeks. Decalcified samples were sectioned and stained with hematoxylin and eosin for histopathological evaluation of synovitis and ankylosis, as

previously described in the literature [25]. The calculated synovitis score was the sum of scores for: enlargement of the synovial lining cell layer (0 points: thickness of 1 layer; 1 point: thickness of 2–3 layers; 2 points: thickness of 4–5 layers; 3 points: thickness of more than 5 layers), density of the resident cells (0 points: normal cellularity; 1 point: slightly increased cellularity; 2 points: moderately increased cellularity; 3 points: greatly increased cellularity, pannus formation and rheumatoid like granulomas might occur) and inflammatory infiltrate (0 points: no inflammatory infiltrate; 1 point: few lymphocytes or plasma cells; 2 points: numerous lymphocytes or plasma cells, sometimes forming follicle-like aggregates; 3 points: dense, band-like inflammatory infiltrate, or numerous large, follicle-like aggregates). The values were summarized and interpreted as follows, 0–1: no synovitis; 2–4: low grade synovitis; 5–9: high grade synovitis. The synovitis score was assessed by two researchers and the kappa coefficient was calculated (*n* = 5 for each group).

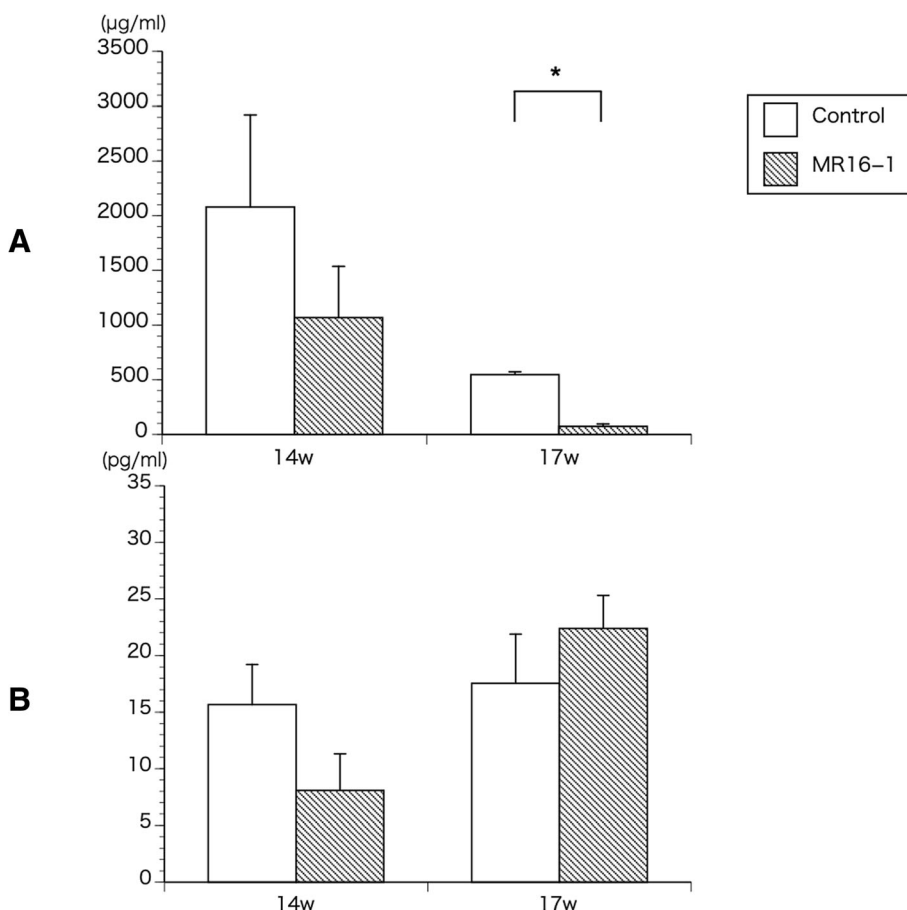


Fig. 1 ELISA assays for SAA and IL-6. **a** ELISA assay for SAA at week 14 and 17. Serum SAA level is significantly lower in MR16-1 treated group at week 17. **b** ELISA assay for IL-6 at week 14 and 17. There is no significant difference in serum IL-6 level. Results are expressed as the mean ± standard error (*n* = 5 mice per group). Representative data are shown from three independent experiments with similar results. **p* < 0.05 by two-way ANOVA with Dunn’s multiple comparison test

Synthesis of indocyanine green liposomes

Indocyanine green (ICG) liposomes were prepared as previously described in the literature [26–28]. Briefly, 1, 2-distearoyl-sn-glycero-3-phosphatidylcholine (DSPC; NOF, Tokyo, Japan) and 1,2-distearoyl-sn-glycero-3-phosphoethanolamine-N-[methoxy-(polyethylene glycol)-2000] (DSPE-PEG[2000-OMe]) (DSPE-PEG:NOF, 94:6 mol/mol) were placed in a pear-shaped flask, and chloroform was added until the lipids were completely dissolved. The chloroform was then evaporated under reduced pressure using a rotary evaporator (NVC-2100/N-1000, Eyela, Tokyo, Japan) until a lipid film remained.

Next, 100 μ M of ICG (Daiichi Sankyo, Tokyo, Japan) dissolved in 10 mL PBS was added to the thin lipid film to form multi-lamellar liposome vesicles. After repeated freeze-thaw cycles, the size of the liposomes was adjusted to < 100 nm using extrusion equipment (Northern Lipids Inc., Vancouver, BC, Canada) with four filter sizes

(100, 200, 400 and 600 nm; Nuclepore Track-Etch Membrane, Whatman plc, Maidstone, UK). For sterilization, liposomes were passed through a 0.45 μ m pore size filter (Millex HV filter unit, Durapore polyvinylidene-difluoride [PVDF] membrane, EMD Millipore, Billerica, MA, USA). Unbound ICG was removed using PD-10 columns. The lipid concentration was measured using the Wako Phospholipids C test (Wako Pure Chemical Industries, Osaka, Japan), and adjusted to 1.0 μ mol/mL. Diameters of the ICG liposomes were measured using a particle size analyzer (ELSZ-2, Otsuka Electronics, Osaka, Japan).

In vivo bioluminescence imaging system analysis

Previous reports indicate that Near-infrared fluorescence imaging system with ICG show significant accumulation in inflamed joints with enhanced permeability and retention (EPR), like as the accumulation observed in tumors

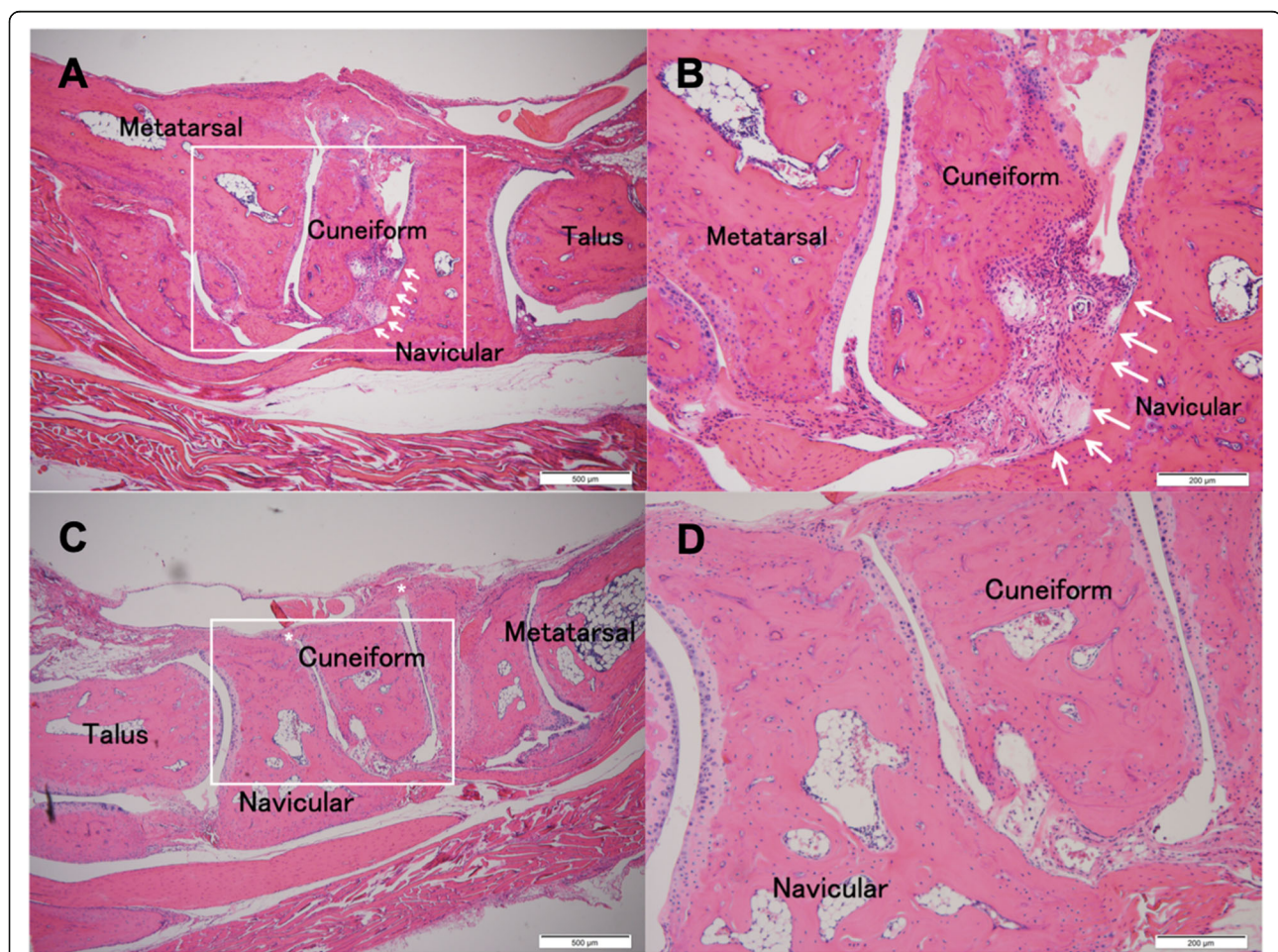
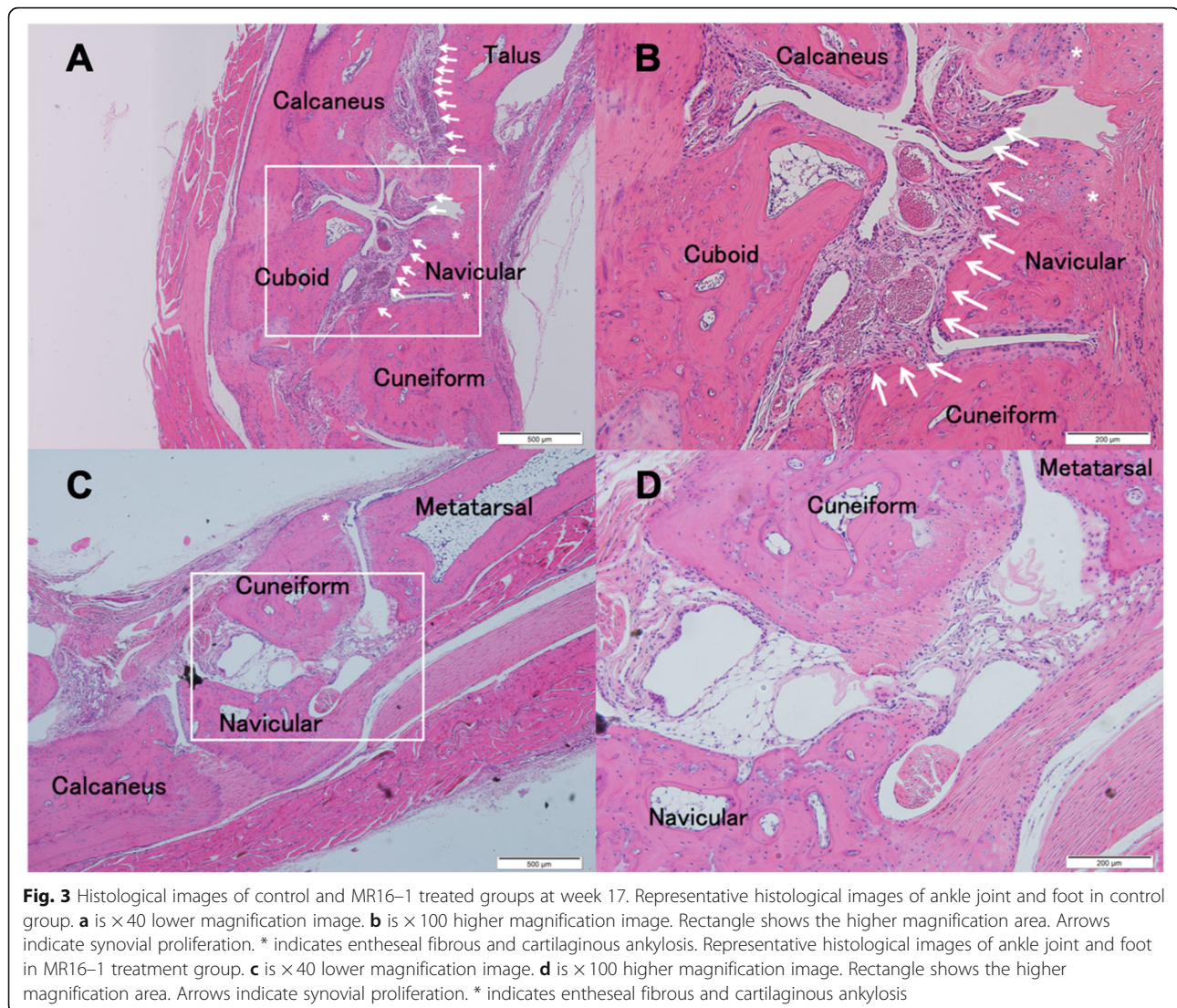


Fig. 2 Histological images of control and MR16-1 treated groups at week 14. Representative histological images of ankle joint and foot in control group. **a** is $\times 40$ lower magnification image. **b** is $\times 100$ higher magnification image. Rectangle shows the higher magnification area. Arrows indicate synovial proliferation. * indicates enthesal fibrous and cartilaginous ankylosis. Representative histological images of ankle joint and foot in MR16-1 treatment group. **c** is $\times 40$ lower magnification image. **d** is $\times 100$ higher magnification image. Rectangle shows the higher magnification area. Arrows indicate synovial proliferation. * indicates fibrous and cartilaginous ankylosis

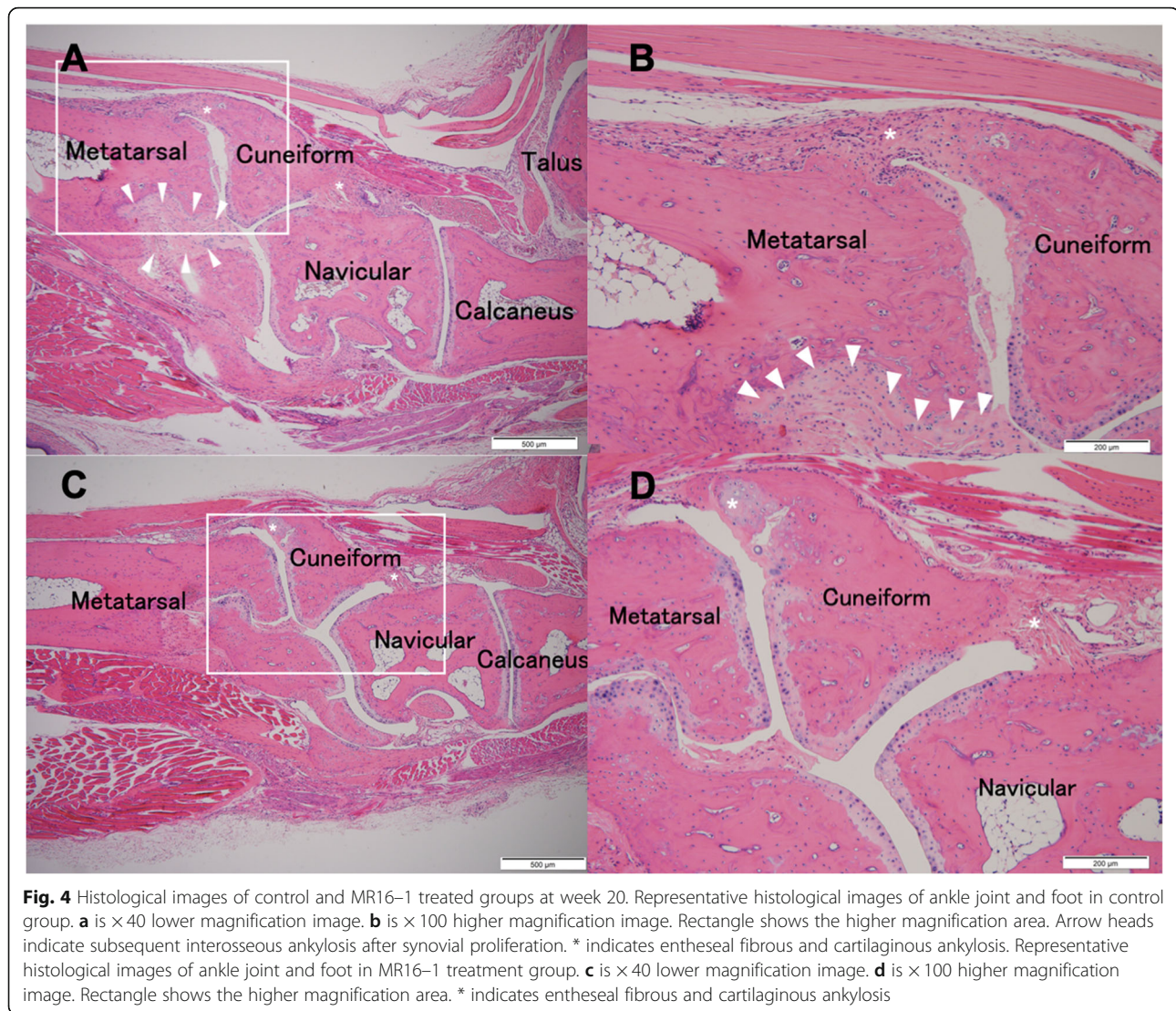


[29, 30]. Blood vessel insufficiency of inflamed joints in arthritic experimental models increases the leakiness and permeability, which enhances the accumulation of liposomes in arthritic lesion by EPR [31]. For the detection of the arthritic inflammation and the proliferation of dysfunctional blood vessels, In vivo bioluminescence imaging system (IVIS) analysis was performed at 10, 14 and 18 weeks of age in MR16-1 treated and control mice ($n = 5$ for each group). Two hundred μL of ICG liposomes was administered intravenously. The fluorescence intensity of leaked ICG was measured at 0, 5, 30, 60, 120 and 180 min after injection using an IVIS; Xenogen, Alameda, CA, USA), as previously described in the literature [26, 27].

Quantitative RT-PCR

Synovial tissue specimens from ankle joints were harvested at 10, 14 and 16 weeks of age ($n = 5$ for each

group). Total RNA was extracted using QIAzol Lysis Reagent (Qiagen, Hilden, Germany) and an RNeasy Mini Kit (Qiagen, Hilden, Germany). Synthesis of cDNA from total RNA was carried out using RT buffer, RT random primers, dNTP mix, and Multiscribe reverse transcriptase (Applied Biosystems, Foster city, CA, USA). A total of $9 \mu\text{L}$ cDNA diluted 1:9 was added to $10 \mu\text{L}$ Taqman Universal Master Mix II with Uracil N-glycosylase (Applied Biosystems, Foster City, CA, USA). Real-time amplification of the genes was performed using $1 \mu\text{L}$ ready-to-use Taqman Gene Expression Assays (Applied Biosystems) for *Il6*, *Tnf*, *IL17*, and *gapdh* as an endogenous control (assay IDs: Mm00446190_m1, Mm00443260_g1, Mm00439618_m1, and Mm99999915_g1). Relative gene expression data were analyzed using the delta-delta-Ct method with PCR-efficiency correction using StepOne software version 2.2.2 (Applied Biosystems), as previously described in the literature [32].



Microcomputed tomography analysis

Microcomputed tomography (micro-CT) imaging was performed at 20 weeks of age ($n = 5$ for each group). Harvested tibiae were stored in 70% ethanol at 4°C, and analyzed using a micro-CT scanner (Scan Xmate-L090; Comscan Techno Co. Ltd., Kanagawa, Japan) operated at a peak voltage of 75 kV and 100 μ A. The scanned region included 505 images from the proximal end of the tibia, at a resolution of 10.4 μ m per voxel, and an image size of 516 \times 506 pixels. Bone volume (BV; mm³), total volume (TV; mm³), bone volume fraction (BV/TV; %) and trabecular thickness (mm) were evaluated and calculated from the axial slice of the proximal tibia using TRI/3D-BON software (Ratoc System Engineering Co., Tokyo, Japan), as previously described in the literature [33].

Statistical analysis

Statistical analyses were performed using JMP software version 13.1 (SAS, Cary, NC, USA). All data are expressed as the mean \pm standard error (SE). Statistical significance of the differences between values were evaluated using the Student's *t*-test, two-way analysis of variance (ANOVA) with Tukey's multiple comparison test and two-way ANOVA with Dunn's multiple comparison test. Values of $p < 0.05$ were regarded as statistically significant. Kappa coefficients were calculated using SPSS version 21 (IBM, Armonk, NY, USA).

Results

ELISA assay

The results of the ELISA assays showed reduced levels of SAA in the MR16-1 treatment group at 14 weeks of age, with significantly decreased levels at week 17 ($p = 0.04$)

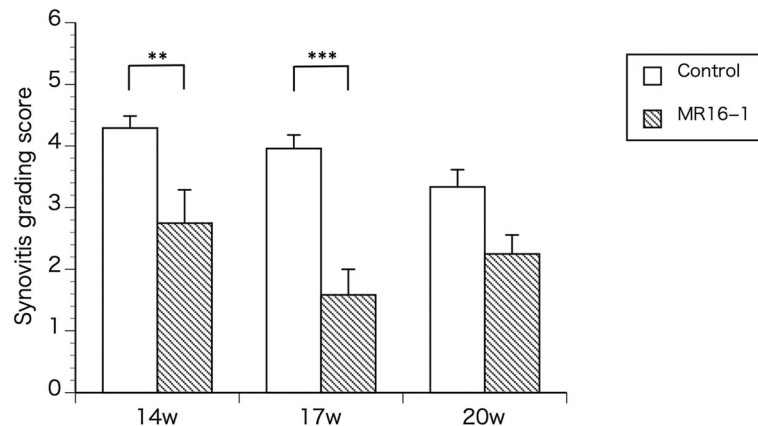


Fig. 5 Histomorphometric analyses with the synovitis grading score of foot and ankle joints in control and MR16-1 treated mice. The synovitis grading scores of MR16-1 treatment group are significantly lower in week 14, 17 and 20 compared with those of control group. Results are expressed as the mean \pm standard error ($n=5$ mice per group). Representative data are shown from three independent experiments with similar results. $**p < 0.01$, $***p < 0.001$ by two-way ANOVA with Tukey's multiple comparison test

(Fig. 1a). The results of the assay for serum IL-6 indicated no significant difference between the control and MR16-1 treatment groups at 14 and 17 weeks of age (Fig. 1b).

Histomorphometric analysis

At 14 weeks of age, control group mice showed apparent synovitis, pannus formation, enthesal inflammation and ankylosis in the ankle region (Fig. 2a and b). In MR16-1 treated mice, synovitis and pannus formation was suppressed compared with the control group

(Fig. 2c and d). At 17 weeks of age, control group mice exhibited acceleration of synovitis, pannus formation and ankle joint ankylosis (Fig. 3a and b). In the MR16-1 treatment group, no synovitis or pannus formation were detected, however, the progression of enthesal inflammatory cells filtration and ankylosis were seen (Fig. 3c and d). At 20 weeks of age, control group mice showed degenerative synovial lesions, advanced pannus formation and joint ankylosing change (Fig. 4a and b). In the MR16-1 treatment group, inflammatory cells

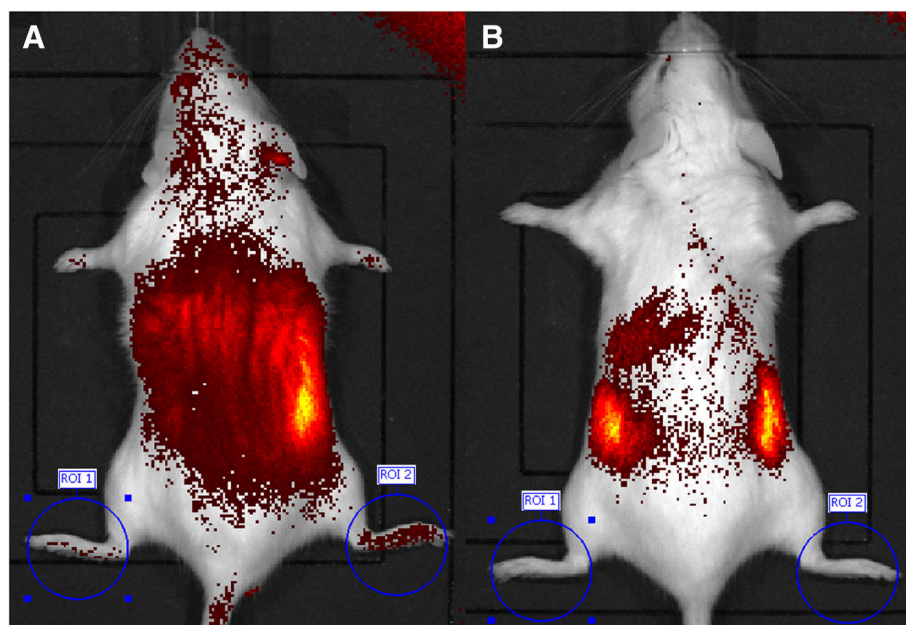


Fig. 6 IVIS analyses in control and MR16-1 treated mice. **a** Representative image of IVIS of control mouse at week 14. There are evident signals in both ankles and feet. **b** Representative image of IVIS of MR16-1 treated mouse at week 14. There are no significant uptake signals in ankles and feet

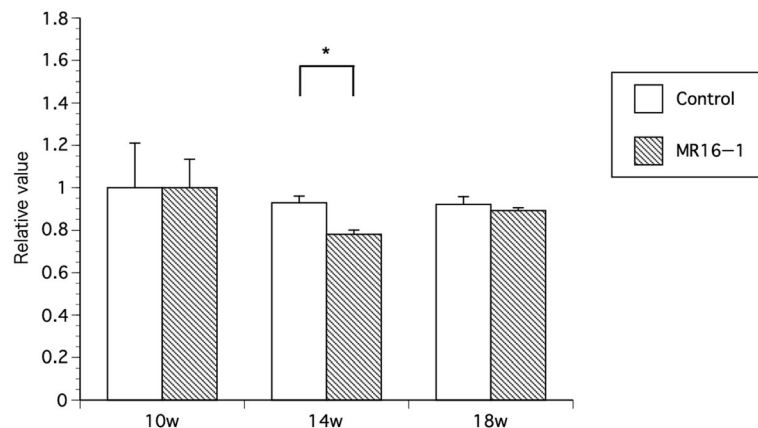


Fig. 7 Quantitative analyses of signal intensity of IVIS at week 10, 14, 18. At week 14, the signal intensity of IVIS of ankles and feet is significantly lower in MR16-1 treatment group, compared with the control group. There are no significant changes in week 10 and 18 in both groups. Results are expressed as the mean \pm standard error ($n = 5$ mice per group). Representative data are shown from three independent experiments with similar results. * $p < 0.05$ by two-way ANOVA with Dunn's multiple comparison test

filtration and ankylosis of the enthesal area were found, although synovitis and pannus formation were absent (Fig. 4c and d). Histopathological assessments of ankle arthritis were performed by calculation of the synovitis score. The Kappa coefficient was calculated to be 0.77, and the reproducibility was good. At week 14, the synovitis score of the control group was 4.29 ± 0.19 , and that of the MR16-1 group was 2.75 ± 0.53 . This indicates a significant difference between the two groups ($p = 0.0098$). At week 17, the synovitis score of the control group was 3.95 ± 0.22 , and that of the MR16-1 group was 1.64 ± 0.27 . This indicates a significant difference between the two groups ($p < 0.001$). At week 20, the synovitis score of the control group was 3.33 ± 0.28 , and that of the MR16-1 group was 2.25 ± 0.3 . This indicates no significant difference between the groups (Fig. 5). Even in the MR16-1 group, the synovitis score was not completely suppressed due to the presence of inflammatory cells filtration of enthesal area.

IVIS analysis

The changes in the signal intensities pre-injection and 120 min after injection were assessed. Representative images of 14 weeks of age control mice and MR16-1 treated mice are shown in Fig. 6a and b. MR16-1 treated mice did not show ICG accumulation in the ankle or foot joints. However, control mice showed obvious accumulation in the foot and ankle joints. The results of IVIS analyses are shown in Fig. 7. Quantitative IVIS was carried out at weeks 10, 14 and 18 in control and MR16-1 treated mice. There was a significant difference in the signal intensities of control and MR16-1 treated mice at week 14 ($p = 0.041$), although there no significant differences were seen at weeks 10 or 18.

Quantitative RT-PCR

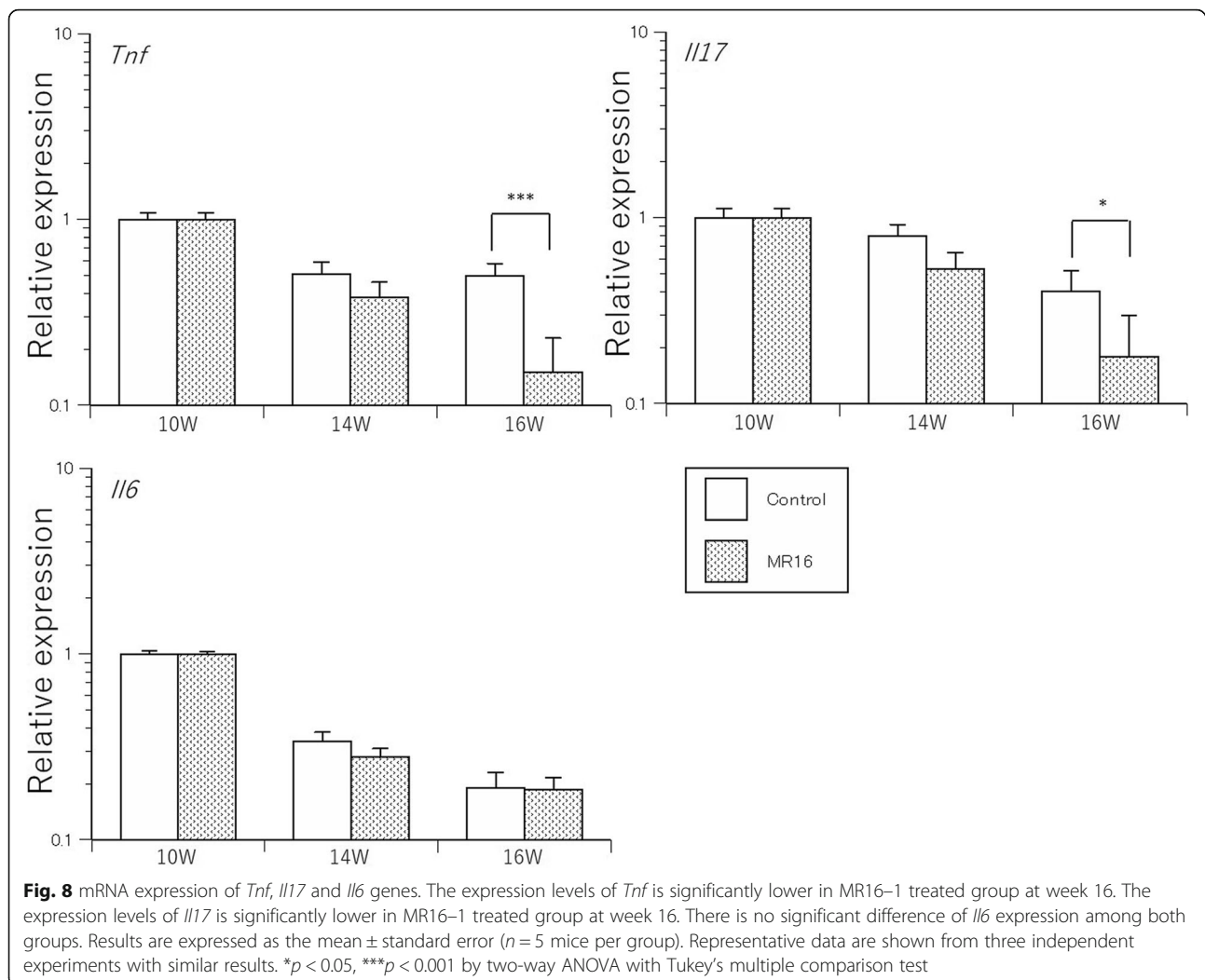
The results of quantitative PCR analyses are shown in Fig. 8. *Tnf* gene expression gradually decreased until week 16 in the MR16-1 treatment group. There was a significant difference in *Tnf* gene expression between the groups at week 16 ($p = 0.001$), which was lower in the MR16-1 treated group than the control group. *Il17* gene expression also gradually decreased until week 16 in the MR16-1 treatment group. There was also a significant difference in *Il17* gene expression between the groups at week 16 ($p = 0.022$), which was lower in MR16-1 treated group. *Il6* gene expression was also evaluated, revealing no significant difference in expression levels between the groups.

Micro CT analysis

In the coronal-reconstructed micro CT images at 20 weeks of age, there were no apparent differences between MR16-1 treatment group and control group mice (Fig. 9a). Quantitative structural analyses of proximal tibia are shown in Fig. 9b. No significant differences were seen in BV, TV, BV/TV or trabecular thickness between the two groups. MR16-1 treatment therefore does not correlate with an increase in bone volume in McH/lpr-RA1 mice.

Discussion

Previous studies have reported several murine models that develop spontaneous ankylosis [34]. For example, DBA/1 mice spontaneously develop ankylosing arthropathy in the ankle joints [35-37]. However, these mice mainly exhibit fibrous proliferation in entheses and fibrous ankylosis, without erosion and bone destruction [34]. Furthermore, other papers reported that the intraperitoneal injection of β -1,3-glucan (curdlan) induced inflammatory arthritis and

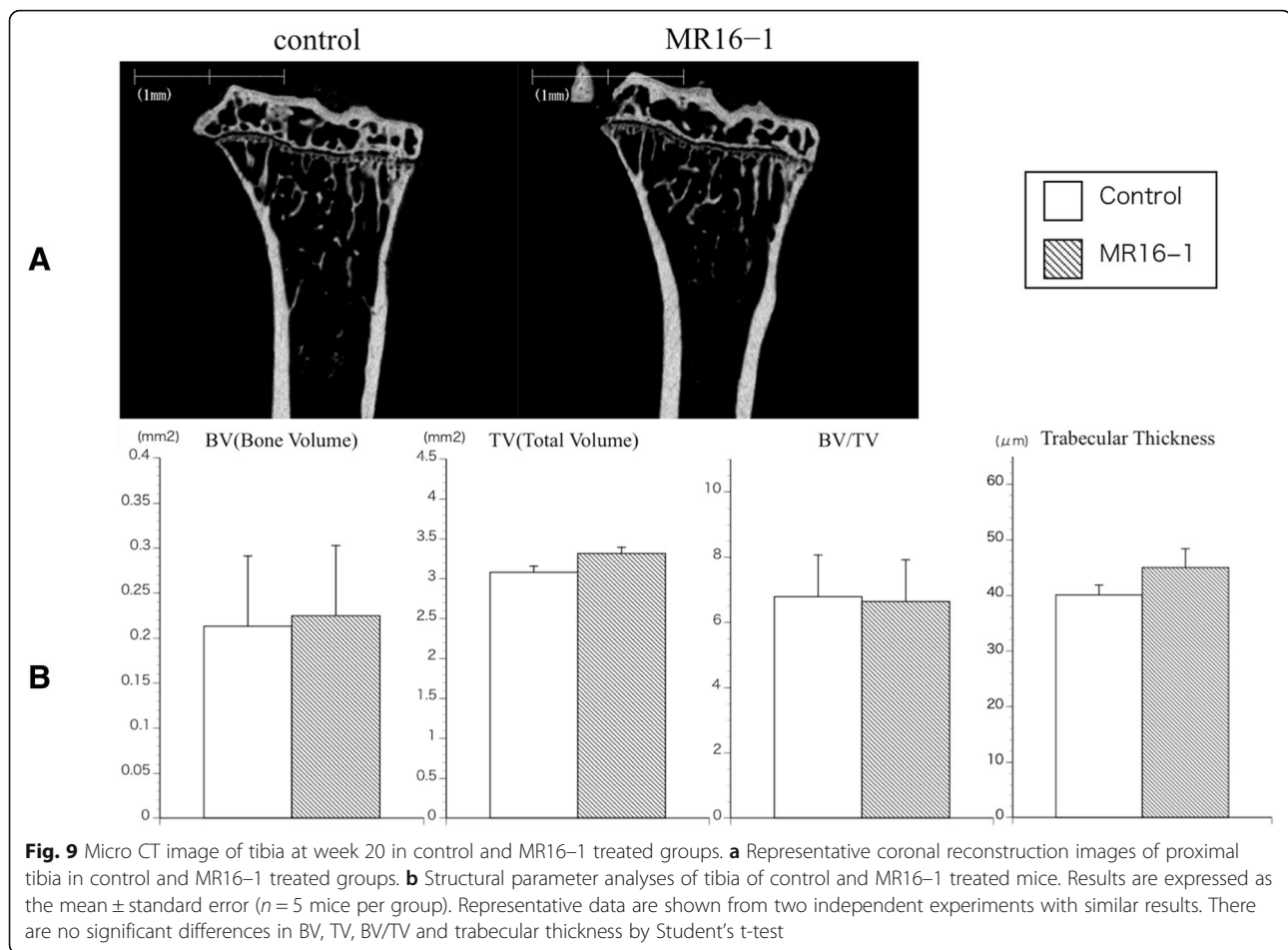


ankylosing spondylitis in SKG mice. These mice indicated dactylitis, enthesitis, synovitis and destructive arthritis [38–40]. SKG mice with the peritoneal injection of curdlan show almost full symptoms of spondyloarthritis. Unlike SKG mice, Mch/lpr-RA1 mice spontaneously show synovitis, pannus formation and enthesal ossification without some specific pathogens [12]. We consider that Mch/lpr-RA1 mice are a suitable experimental disease model of peripheral arthritis in spondyloarthritis. The present study explores the effects of treatment with the anti-IL-6 receptor monoclonal antibody in Mch/lpr-RA1 mice. In the MR16-1 treated group, results of histomorphometric and IVIS analyses showed that the proliferation of synovium and joint destruction were suppressed. However, histological investigations confirmed that enthesal ossification and ankylosis progressed even with IL-6 blockade treatment. We propose that the anti-IL-6 receptor antibody contributes to the suppression of synovial proliferation and bone destruction in Mch/lpr-RA1 mice,

but that further factors are involved in the prevention of enthesal inflammation and ossification.

Changes in the bone parameters of MR16-1 treated and control mice were evaluated by micro-CT imaging. In this study there were no significant differences in the bone parameters between two groups. Published studies reported the treatment effects of MR16-1 to include increased bone volume and bone strength in DBA/1 mice with collagen-induced arthritis [22, 41]. However, in this study Mch/lpr-RA1 mice did not show increased bone volume following MR16-1 treatment. In the published study, the dose of MR16-1 was much higher — 8 mg was administered to DBA/1 mice. Our different findings of the effect of MR16-1 treatment on bone volume were likely due to the different dosage of MR16-1.

SAA is related with the pathogenesis of rheumatoid arthritis, and previous reports indicated that SAA was linked to disease activity and treatment response of rheumatoid arthritis [42, 43]. SAA is a suitable acute



phase reactant of mice [44, 45], and previous studies showed that MR16-1 treatment suppressed the expression level serum SAA [21, 46]. SAA can be a relevant inflammation marker and useful for predicting the treatment response in the arthritis and enthesitis in Mch/lpr-RA1 mice. SAA was significantly lower in the MR16-1 treated group, and we consider that the dose of MR16-1 that was administered is sufficient to suppress inflammation in Mch/lpr-RA1 mice. MR16-1 is an anti-IL-6 receptor antibody for the treatment, so it is unsurprising that there were no changes in serum IL-6 level. The results of quantitative RT-PCR showed that gene expression levels of *tnf* and *IL17* were suppressed by IL-6 signal blockade. Previous studies reported that IL-6 signal blockade by MR16-1 suppresses IL-17 signaling [47, 48]. Suppression of IL-6, TNF- α and IL-17 signals may contribute to the prevention of synovitis and bone destruction in Mch/lpr-RA1 mice. However, only partial prevention of enthesal ossification and joint ankylosis were seen in the MR16-1 treated group — at week 20 the histological images showed the progression of histological findings of enthesal ossification and ankylosis, regardless of the prevention of synovial proliferation and

bone destruction. In the results of previous clinical trials, administration of anti-IL-6 receptor antibody was insufficient for complete treatment of ankylosing spondylitis [14]. Some studies have reported that enthesal ossification in spondyloarthritis is related to IL-17 signaling [49]. The blockade of IL-17 signaling was achieved in this study; however, this signal suppression might be insufficient, as other signaling pathways (such as IL-12, IL-22 and IL-23) could be involved in the mechanisms of enthesal ossification and ankylosis. Further studies should be performed to assess the effects of IL-12, IL-22 and IL-23 signaling blockade for treatment of enthesal ossification and ankylosis with Mch/lpr-RA1 mice. We consider that Mch/lpr-RA1 is a useful animal model of peripheral spondyloarthritis, and a promising tool for the evaluation and development of new treatment reagents and drug repositioning treatment in destructive arthritis and enthesal inflammation. SKG mice with the peritoneal injection of curdlan seem to be a suitable animal model of spondyloarthritis, nevertheless the evaluation and development of new treatment reagents should be assessed in different strains of mice models, including Mch/lpr-RA1 mice.

The results of IVIS analyses showed that there was a significant difference between the two groups in week 14 only. These results are inconsistent with the results of histological analyses, PCR and ELISA of SAA, which indicated significant differences after week 14. We consider that the proliferation of dysfunctional blood vessels in inflamed joints of McH/lpr-RA1 mice decreases around week 18. The histological findings showed significant differences and advanced deformity in late phase arthritis, including bone erosion, pannus formation and ankylosis. The advancement of destructive arthritis and ankylosis after the decreased formation of dysfunctional blood vessels may induce the inconsistent results of IVIS and histological synovitis score.

Conclusion

In the present study, we have demonstrated for the first time that IL-6 signal blockade with MR16-1 significantly reduces the development of synovitis and joint destruction in the murine experimental model of spontaneous arthritis and enthesitis, McH/lpr-RA1. Our results indicate that the progression of deformity associated with enthesal ossification continue even with anti-IL-6 receptor antibody treatment; indicating that further factors might be involved in the progression of enthesal ossification. McH/lpr-RA1 is a promising animal model for the elucidation of the mechanism of destructive arthritis and enthesitis, and development of new treatment.

Abbreviations

BV: Bone volume; cDNA: complementary DNA; CT: Computed tomography; ELISA: Enzyme-linked immunosorbent assay; ICG: Indocyanine green; IL: Interleukin; IVIS: In vivo bioluminescence imaging system; PBS: Phosphate-buffered saline; RT-PCR: Realtime polymerase chain reaction; SAA: Serum amyloid A; TNF: Tumor necrosis factor; TV: Total volume

Acknowledgements

We thank DR. Amy Phillips for editing a draft of this manuscript.

Authors' contributions

Conceived and designed the experiments: TI, YM, SM, TK. Performed the experiments: TI, YM. Contributed materials/analysis tools: YM, SM, TK. Wrote the manuscript: TI, YM, NM, EI. All authors have read and approved the manuscript.

Funding

This study was supported by JSPS KAKENHI (18 K09052). The funder had no role in study design, data collection and analysis, decision to publish, or preparation of the manuscript.

Availability of data and materials

The datasets generated and/or analyzed during the current study are available from the corresponding author on reasonable request.

Ethics approval and consent to participate

Experiments were approved by The Tohoku University Animal Studies Ethics Committee.

Consent for publication

Not applicable.

Competing interests

The authors declare that they have no competing interests.

Author details

¹Department of Orthopaedic Surgery, Tohoku University Graduate School of Medicine, 1-1, Seiryomachi, Aoba-ku, Sendai, Miyagi 980-8574, Japan.

²Laboratory of Biomedical Engineering for Cancer, Department of Biomedical Engineering, Graduate School of Biomedical Engineering, Tohoku University, 4-1, Seiryomachi, Aoba-ku, Sendai, Miyagi 980-8575, Japan. ³Department of Diagnostic Radiology, Tohoku University Graduate School of Medicine, 1-1, Seiryomachi, Aoba-ku, Sendai, Miyagi 980-8574, Japan.

Received: 19 September 2018 Accepted: 4 June 2019

Published online: 15 June 2019

References

- Ronneberger M, Schett G. Pathophysiology of Spondyloarthritis. *Curr Rheumatol Rep*. 2011;13(5):416–20.
- Scott DL, Wolfe F, Huizinga TW. Rheumatoid arthritis. *Lancet*. 2010;376(9746):1094–108.
- Benjamin M, McGonagle D. The anatomical basis for disease localisation in seronegative spondyloarthropathy at entheses and related sites. *J Anat*. 2001;199:503–26.
- Paramarta JE, van der Leij C, Gofita I, Yerenenko N, van de Sande MG, de Hair MJ, et al. Peripheral joint inflammation in early onset spondyloarthritis is not specifically related to enthesitis. *Ann Rheum Dis*. 2014;73(4):735–40.
- Lories RJU, Matthys P, de VK, Derese I, Luyten FP. Ankylosing enthesitis, dactylitis, and onychopariostitis in male DBA/1 mice: a model of psoriatic arthritis. *Ann Rheum Dis*. 2004;63(5):595–8.
- Oishi H, Miyazaki T, Mizuki S, Kamogawa J, Lu L-M, Tsubaki T, et al. Accelerating effect of an MRL gene locus on the severity and onset of arthropathy in DBA/1 mice. *Arthritis Rheum*. 2005;52(3):959–66.
- Reinhardt A, Yevsa T, Worbs T, Lienenklaus S, Sandrock I, Oberdörfer L, et al. Interleukin-23-dependent $\gamma\delta$ T cells produce Interleukin-17 and accumulate in the Enthesis, aortic valve, and ciliary body in mice. *Arthritis Rheumatol*. 2016;68(10):2476–86.
- Sherlock JP, Joyce-Shaikh B, Turner SP, Chao C-C, Sathé M, Grein J, et al. IL-23 induces spondyloarthropathy by acting on ROR- γ t+ CD3+CD4–CD8– enthesal resident T cells. *Nat Med*. 2012;18(7):1069–76.
- Baraliakos X, Heldmann F, Callhoff J, Listing J, Appelboom T, Brandt J, et al. Which spinal lesions are associated with new bone formation in patients with ankylosing spondylitis treated with anti-TNF agents? A long-term observational study using MRI and conventional radiography. *Ann Rheum Dis*. 2014;73(10):1819–25.
- Weiβ A, Song I-H, Haibel H, Listing J, Sieper J. Good correlation between changes in objective and subjective signs of inflammation in patients with short- but not long duration of axial spondyloarthritis treated with tumor necrosis factor-blockers. *Arthritis Res Ther*. 2014;16(1):R35.
- Zhang J-R, Liu X-J, Xu W-D, Dai S-M. Effects of tumor necrosis factor- α inhibitors on new bone formation in ankylosing spondylitis. *Joint Bone Spine*. 2016;83(3):257–64.
- Mori S, Tanda N, Ito MR, Oishi H, Tsubaki T, Komori H, et al. Novel recombinant congenic mouse strain developing arthritis with enthesopathy. *Pathol Int*. 2008;58(7):407–14.
- Teitsma XM, Marijnissen AKA, Bijlsma JWJ, Lafeber FJP, Jacobs JWG. Tocilizumab as monotherapy or combination therapy for treating active rheumatoid arthritis: a meta-analysis of efficacy and safety reported in randomized controlled trials. *Arthritis Res Ther*. 2016;18(1):211.
- Sieper J, Porter-Brown B, Thompson L, Harari O, Dougados M. Assessment of short-term symptomatic efficacy of tocilizumab in ankylosing spondylitis: results of randomised, placebo-controlled trials. *Ann Rheum Dis*. 2014;73(1):95–100.
- Lekpa F, Poulain C, Wendling D, Soubrier M, De Bandt M, Berthelot J, et al. Is IL-6 an appropriate target to treat spondyloarthritis patients refractory to anti-TNF therapy? A multicentre retrospective observational study. *Arthritis Res Ther*. 2012;14(2):R53.
- Mihara M, Takagi N, Takeda Y, Ohsugi Y. IL-6 receptor blockage inhibits the onset of autoimmune kidney disease in NZB/W F1 mice. *Clin Exp Immunol*. 1998;112(3):397–402.
- Arima H, Hanada M, Hayasaka T, Masaki N, Omura T, Xu D, et al. Blockade of IL-6 signaling by MR16-1 inhibits reduction of docosahexaenoic acid-containing phosphatidylcholine levels in a mouse model of spinal cord injury. *Neuroscience*. 2014;269:1–10.

18. Birner P, Heider S, Petzelbauer P, Wolf P, Kornauth C, Kuroll M, et al. Interleukin-6 receptor alpha blockade improves skin lesions in a murine model of systemic lupus erythematosus. *Exp Dermatol*. 2016;25(4):305–10.
19. Iwanami K, Matsumoto I, Tanaka-Watanabe Y, Inoue A, Mihara M, Ohsugi Y, et al. Crucial role of the interleukin-6/interleukin-17 cytokine axis in the induction of arthritis by glucose-6-phosphate isomerase. *Arthritis Rheum*. 2008;58(3):754–63.
20. Ohtsuiji M, Lin Q, Nishikawa K, Ohtsuiji N, Okazaki H, Tsurui H, et al. IL-6 signal blockade ameliorates the enhanced osteoclastogenesis and the associated joint destruction in a novel FcγRIIB-deficient rheumatoid arthritis mouse model. *Mod Rheumatol*. 2015;25(2):270–7.
21. Suzuki M, Yoshida H, Hashizume M, Tanaka K, Matsumoto Y. Blockade of interleukin-6 receptor enhances the anti-arthritis effect of glucocorticoids without decreasing bone mineral density in mice with collagen-induced arthritis. *Clin Exp Immunol*. 2015;182(2):154–61.
22. Yoshida H, Suzuki M, Tanaka K, Takeda S, Yogo K, Matsumoto Y. Anti-interleukin-6 receptor antibody prevents loss of bone structure and bone strength in collagen-induced arthritis mice. *Scand J Rheumatol*. 2018;47(5):384–91.
23. Latourte A, Cherifi C, Maillat J, Ea H-K, Bouaziz W, Funck-Brentano T, et al. Systemic inhibition of IL-6/Stat3 signalling protects against experimental osteoarthritis. *Ann Rheum Dis*. 2017;76(4):748–55.
24. Yoshida H, Hashizume M, Suzuki M, Mihara M. Induction of high-dose tolerance to the rat anti-mouse IL-6 receptor antibody in NZB/NZW F1 mice. *Rheumatol Int*. 2011;31(11):1445–9.
25. Krenn V, Morawietz L, Burmester G-R, Kinne RW, Mueller-Ladner U, Muller B, et al. Synovitis score: discrimination between chronic low-grade and high-grade synovitis. *Histopathology*. 2006;49(4):358–64.
26. Kato S, Mori S, Kodama T. A novel treatment method for lymph node metastasis using a lymphatic drug delivery system with Nano/microbubbles and ultrasound. *J Cancer*. 2015;6(12):1282–94.
27. Mikada M, Sukhbaatar A, Miura Y, Horie S, Sakamoto M, Mori S, et al. Evaluation of the enhanced permeability and retention effect in the early stages of lymph node metastasis. *Cancer Sci*. 2017;108(5):846–52.
28. Kodama T, Tomita N, Horie S, Sax N, Iwasaki H, Suzuki R, et al. Morphological study of acoustic liposomes using transmission electron microscopy. *J Electron Microscop*. 2010;59(3):187–96.
29. Onishi S, Sakane M, Tsukanishi T, Funayama T, Ozeki E, Hara I, et al. Near-infrared fluorescence imaging with indocyanine green-lactosomes in a mouse model of rheumatoid arthritis. *Mod Rheumatol*. 2016;26(6):885–90.
30. Wu H, Wu H, He Y, Gan Z, Xu Z, Zhou M, et al. Synovitis in mice with inflammatory arthritis monitored with quantitative analysis of dynamic contrast-enhanced NIR fluorescence imaging using iRGD-targeted liposomes as fluorescence probes. *Int J Nanomedicine*. 2018;13:1841–50.
31. Kennedy A, Ng CT, Biniecka M, Saber T, Taylor C, O'Sullivan J, et al. Angiogenesis and blood vessel stability in inflammatory arthritis. *Arthritis Rheum*. 2010;62(3):711–21.
32. Fujisawa H, Mori Y, Kogure A, Tanaka H, Kamimura M, Masahashi N, et al. Effects of intramedullary nails composed of a new β-type Ti-Nb-Sn alloy with low Young's modulus on fracture healing in mouse tibiae. *J Biomed Mater Res B Appl Biomater*. 2018;106:2841–8.
33. Kamimura M, Mori Y, Sugahara-Tobinai A, Takai T, Itoi E. Impaired fracture healing caused by deficiency of the Immunoreceptor adaptor protein DAP12. *PLoS One*. 2015. <https://doi.org/10.1371/journal.pone.0128210>.
34. Breban M, Araujo LM, Chiochia G. Editorial: animal models of Spondyloarthritis: do they faithfully Mirror human disease? *Arthritis Rheumatol*. 2014;66(7):1689–92.
35. Holmdahl R, Jansson L, Andersson M, Jonsson R. Genetic, hormonal and behavioural influence on spontaneously developing arthritis in normal mice. *Clin Exp Immunol*. 1992;88(3):467–72.
36. Nordling C, Karlsson-Parra A, Jansson L, Holmdahl R, Klareskog L. Characterization of a spontaneously occurring arthritis in male DBA/1 mice. *Arthritis Rheum*. 1992;35(6):717–22.
37. Weinreich S, Capkova J, Hoebe-Hewryk B, Boog C, Ivanyi P. Grouped caging predisposes male mice to ankylosing enthesopathy. *Ann Rheum Dis*. 1996;55(9):645–7.
38. Benham H, Rehaume LM, Hasnain SZ, Velasco J, Baillet AC, Ruutu M, et al. Interleukin-23 mediates the intestinal response to microbial β-1,3-glucan and the development of Spondyloarthritis pathology in SKG mice. *Arthritis Rheumatol*. 2014;66(7):1755–67.
39. Lau MC, Keith P, Costello M-E, Bradbury LA, Hollis KA, Thomas R, et al. Genetic association of ankylosing spondylitis with TBX21 influences T-bet and pro-inflammatory cytokine expression in humans and SKG mice as a model of spondyloarthritis. *Ann Rheum Dis*. 2017;76(1):261–9.
40. Ruutu M, Thomas G, Steck R, Degli-Esposti MA, Zinkernagel MS, Alexander K, et al. β-Glucan triggers spondylarthritis and Crohn's disease-like ileitis in SKG mice. *Arthritis Rheum*. 2012;64(7):2211–22.
41. Tanaka K, Hashizume M, Mihara M, Yoshida H, Suzuki M, Matsumoto Y. Anti-interleukin-6 receptor antibody prevents systemic bone mass loss via reducing the number of osteoclast precursors in bone marrow in a collagen-induced arthritis model: anti-IL-6R antibody prevents systemic bone mass loss. *Clin Exp Immunol*. 2014;175(2):172–80.
42. Connolly M, Mullan RH, McCormick J, Matthews C, Sullivan O, Kennedy A, et al. Acute-phase serum amyloid A regulates tumor necrosis factor α and matrix turnover and predicts disease progression in patients with inflammatory arthritis before and after biologic therapy. *Arthritis Rheum*. 2012;64(4):1035–45.
43. Visvanathan S, Wagner C, Rojas J, Kay J, Dasgupta B, Matteson EL, et al. E-selectin, interleukin 18, serum amyloid A, and matrix metalloproteinase 9 are associated with clinical response to Golimumab plus methotrexate in patients with active rheumatoid arthritis despite methotrexate therapy. *J Rheumatol*. 2009;36(7):1371–9.
44. Le PT, Muller MT, Mortensen RF. Acute phase reactants of mice. I. Isolation of serum amyloid P-component (SAP) and its induction by a monokine. *J Immunol*. 1982;129(2):665–72.
45. Petersen HH, Nielsen JP, Heegaard PMH. Application of acute phase protein measurements in veterinary clinical chemistry. *Vet Res*. 2004;35(2):163–87.
46. Mihara M, Shiina M, Nishimoto N, Yoshizaki K, Kishimoto T, Akamatsu K. Anti-interleukin 6 receptor antibody inhibits murine AA-amyloidosis. *J Rheumatol*. 2004;31(6):1132–8.
47. Hashimoto-Kataoka T, Hosen N, Sonobe T, Arita Y, Yasui T, Masaki T, et al. Interleukin-6/interleukin-21 signaling axis is critical in the pathogenesis of pulmonary arterial hypertension. *Proc Natl Acad Sci U S A*. 2015;112(20):E2677–86.
48. Hirota K, Hashimoto M, Yoshitomi H, Tanaka S, Nomura T, Yamaguchi T, et al. T cell self-reactivity forms a cytokine milieu for spontaneous development of IL-17+ Th cells that cause autoimmune arthritis. *J Exp Med*. 2007;204(1):41–7.
49. Speeckaert R, van Geel N, Lambert J, Claeys L, Delanghe JR, Speeckaert MM. Secukinumab: IL-17A inhibition to treat psoriatic arthritis. *Drugs Today*. 2016; 52(11):607–16.

Publisher's Note

Springer Nature remains neutral with regard to jurisdictional claims in published maps and institutional affiliations.

Ready to submit your research? Choose BMC and benefit from:

- fast, convenient online submission
- thorough peer review by experienced researchers in your field
- rapid publication on acceptance
- support for research data, including large and complex data types
- gold Open Access which fosters wider collaboration and increased citations
- maximum visibility for your research: over 100M website views per year

At BMC, research is always in progress.

Learn more biomedcentral.com/submissions

